Journal of Marine Science and Application (2019) 18:205–212
https://doi.org/10.1007/s11804-019-00078-6

RESEARCH ARTICLE

Analysis of Capability Requirement of Dynamic Positioning System for Cargo Transfer Vessel at Sea

Kaiye Hu[1] · Yong Ding[1] · Hongwei Wang[1] · Dapeng Xiong[1] · Di Yang[1]

Received: 18 October 2017 / Accepted: 16 June 2018 / Published online: 4 March 2019

Abstract

In response to the development of deep-sea oil and gas resources, which require a high degree of cooperation by crude oil transportation equipment, a new type of ship known as the cargo transfer vessel (CTV) has been developed. To provide a theoretical reference for the design and equipment of the CTV's dynamic positioning system, in this paper, we take the new deepwater CTV as the study object and theoretically and numerically analyze its operation, wind load, current load, wave load, and navigational resistance in a range of Brazilian sea conditions with respect to its positioning and towing modes. We confirm that our proposed method can successfully calculate the total environmental load of the CTV and that the CTV is able to operate normally under the designed sea conditions.

Keywords Cargo transfer vessel · Wind load · Current load · Wave load · DP capability · Oil transfer operation

1 Introduction

In recent years, as the production of offshore oil and gas resources has continued to expand, the number of floating production storage and offloading (FPSO) vessels has rapidly increased, as has the demand for crude oil transportation equipment, which is an important component of the FPSO oil unloading system. Deep-sea oil and gas resources development requires a high degree of cooperation by crude oil transportation equipment, and the presence of all this equipment can restrict the deep-sea oil exploration. At present, a shuttle tanker is used to transport oil from the FPSO to the port. However, compared with ordinary tankers, the shuttle tanker is small and its running costs are very high. Therefore, determining how to use an ordinary tanker in crude oil transfer operations has become an urgent technical requirement.

Article Highlights
- To calculate the capability requirements of the dynamic positioning system of the CTV, the typical operation mode of the CTV is analyzed.
- A method for calculating the environment load is proposed and applied.
- The environmental load in different operational modes is calculated.

✉ Kaiye Hu
hukaiye@hrbeu.edu.cn

[1] College of Shipbuilding Engineering, Harbin Engineering University, Harbin 150001, China

In this scenario, the cargo transfer vessel (CTV) came into being. The CTV is a new concept in deepwater high-power crude oil delivery equipment. At the same time, a new crude oil transfer operation concept was introduced, known as the "FPSO + CTV + ordinary tanker" mode. In this mode, a very large crude carrier (VLCC) is towed by a CTV equipped with a dynamic positioning device to a position nearby an FPSO. Through a large-diameter pipeline, the crude oil is transferred from the FPSO to the CTV and the CTV unloads the crude oil into the VLCC. This crude oil export mode is an international initiative and has the advantages of being more cost-effective, safe, and reliable.

The CTV has proven to have good self-propulsion and flexibility of movement. The main function of the CTV is crude oil delivery, and it has very strict requirements for the positioning capacity of its hull.

With respect to conventional offshore engineering floating bodies, many scholars have analyzed the dynamic positioning (DP) requirements (Mahfouz and Eltahan 2006; Mahfouz 2007; Zhang and Yang 2009; Fu et al. 2010; Sun et al. 2011; Liu et al. 2016; Li and Ren 2018; Wang et al. 2018). Bao (2018) performed a time domain analysis of a platform DP system. Experimental investigations of the DP system have been conducted by Tannuri and Morishita (2006), Wu et al. (2016), Xu et al. (2016), Zhao et al. (2010), and Xu et al. (2011). Zhao (2018) studied the thruster allocation algorithm for a DP system. Do (2011), Kjerstad and Skjetne (2014), Liang et al. (2015), Zhang et al. (2016), Lin et al. (2018),

Fig. 1 Cargo transfer vessel

and Xin and Du (2018) researched control methods for DP systems.

The CTV operation mode differs from that of a conventional offshore vessel. In this study, we consider the typical CTV operating mode and analyze its positioning capability requirements to ensure that the CTV can meet its positioning requirements under the designed sea conditions. The results of this work are applicable to the CTV DP system design and projects related to the development of oil and gas resources in deep-sea conditions.

Table 1 Marine environmental parameters

Significant wave height/m	Peak spectral period/s	Wave spectra	γ	Maximum wind speed (above sea level 10 m)/ ($m \cdot s^{-1}$)	Maximus current speed/ ($m \cdot s^{-1}$)
4.0	8.0	JONSWAP	3.3	17.1	1.0

2 Typical CTV Operating Mode

Figure 1 shows an external view of a CTV. In actual operation, an FPSO is fixed by a multi-point mooring system such that the position and direction do not change with the presence of an external load, and the orientations of the CTV and VLCC depend on the direction of the wind waves. Figure 2 shows

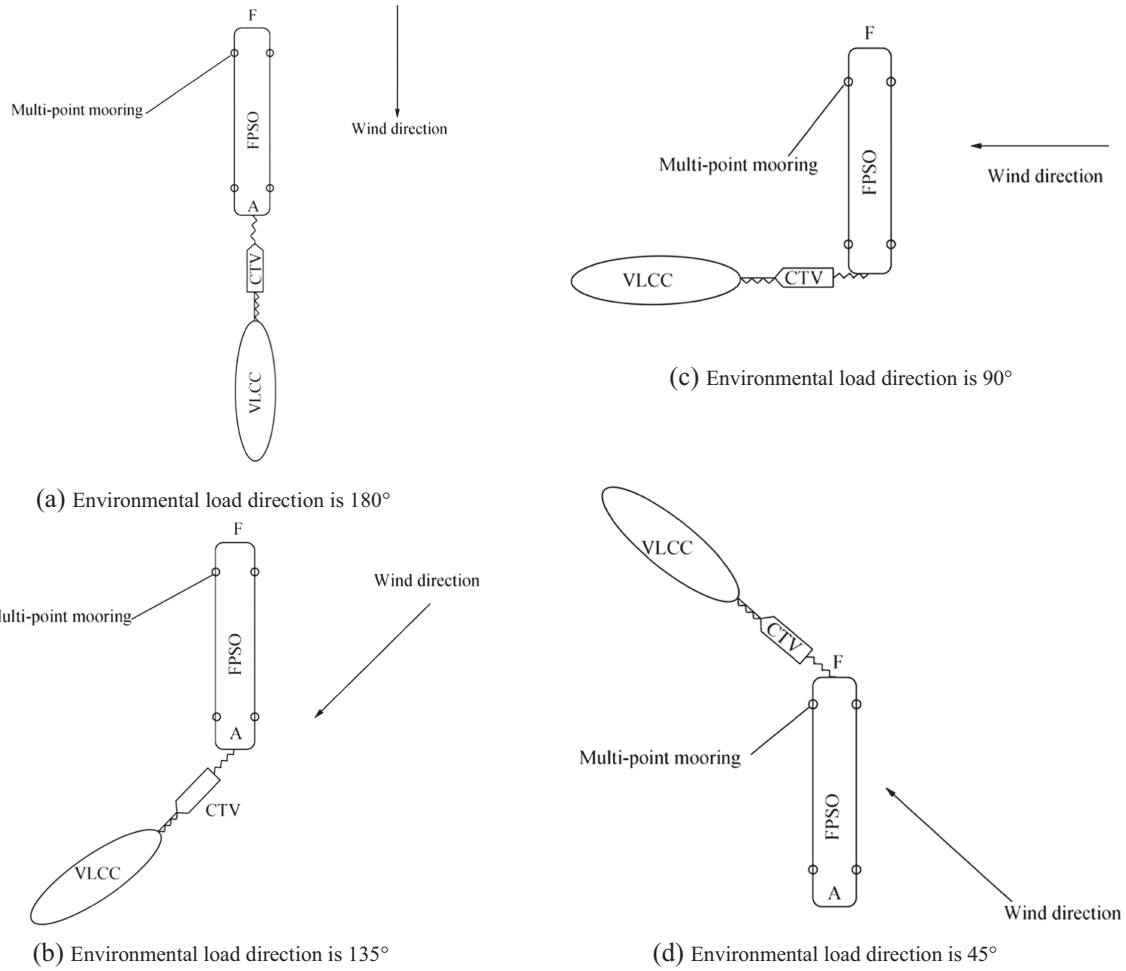

Fig. 2 Typical CTV operating mode. **a** Environmental load direction is 180°. **b** Environmental load direction is 135°. **c** Environmental load direction is 90°. **d** Environmental load direction is 45°

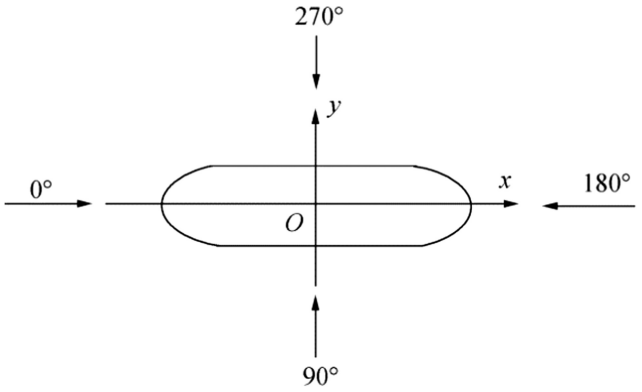

Fig. 3 Coordinate system

Therefore, it is important to determine the ultimate load on the CTV in typical sea conditions. Using statistical data for the CTV sea area, we select typical sea conditions in the Brazilian sea, for which Table 1 shows the marine environmental parameters. Taking into account the complexity of the environment, we set the wind, current, and wave loads to come from the same direction, and do not consider any coupling between the three.

In the analysis of the CTV's external load, a unified hull coordinate system is required. In this paper, we set the coordinates of the origin at midship and define the direction from the load point to the stern as 0° and the bow direction as 180°, as shown in Fig. 3.

Table 2 Lateral projection area of component A_T

Components	Superstructure	Crane 1	Crane 2	Crane 3	Crane 4	Winch
A_T/m^2	221.32	4.368	4.368	4.368	4.368	241.6

four typical operating modes, where F indicates the bow side and A the aft side. The direction from aft to bow is 0°, the curve indicates the oil delivery pipe, and the line indicates the cable.

From the figure, we can see that when the external load direction ranges between 90° and 180° and the CTV connects the oil pipeline to the stern of the FPSO and tows the VLCC to the stern side of the FPSO. If there is a sudden change in the environmental load direction of 90° or more, the CTV must tow the VLCC to the FPSO bow side for reconnection with the tubing and pulls the VLCC to the side of the FPSO bow. As shown in Fig. 2, the CTV and VLCC are always in the upwind position regardless of the directions of the wind and waves. The conditions shown in Fig. 2 d and b are essentially the same.

From the above analysis, we know that the CTV serves as a transfer vessel from the FPSO to the tanker. A DP system is used to manage the environmental load and control the location of the CTV's area of operation while also controlling the position of the CTV between the FPSO and tanker. This prevents collision and achieves the FPSO crude oil transfer to the VLCC. Therefore, the CTV's DP capability is a critical factor.

3 Analysis of CTV DP Capability

In this paper, we focus on the maximum demand on the CTV DP capability, that is, the maximum thrust that a CTV requires for each application mode (Fossen 1994; Yang 2018).

3.1 Wind Load

In this paper, we use the DP analysis guide developed by the IMCA, and divided the CTV into two parts, i.e., the main hull and the superstructure. For the main hull calculations, we used the wind coefficient method, and for the superstructure, we used the modular method. We then superimposed the two to obtain the longitudinal and transverse wind loads. We obtained the wind loads from other wind directions by interpolation.

For the main hull, we used the following formula in our calculations:

$$\begin{cases} F_{\mathrm{wd}x}(\mathrm{hull}) = \dfrac{1}{2}\rho v_{\mathrm{wd}}^2 C_{\mathrm{wd}x}(\partial) A_{\mathrm{T}}(\mathrm{hull}) \\ F_{\mathrm{wd}y}(\mathrm{hull}) = \dfrac{1}{2}\rho v_{\mathrm{wd}}^2 C_{\mathrm{wd}y}(\partial) A_{\mathrm{L}}(\mathrm{hull}) \\ F_{\mathrm{wd}z}(\mathrm{hull}) = \dfrac{1}{2}\rho v_{\mathrm{wd}}^2 C_{\mathrm{wd}z}(\partial) A_L(\mathrm{hull}) L_{\mathrm{pp}} \end{cases} \quad (1)$$

where $F_{\mathrm{wd}x}$(hull), $F_{\mathrm{wd}y}$(hull), and $F_{\mathrm{wd}z}$(hull) are the longitudinal wind load, transverse wind load, and bow wind load of the main hull, respectively; ∂ is the wind direction angle; A_{T}(hull) and A_{L}(hull) are the transverse and longitudinal cross-sectional areas of the hull; ρ is the density of the air; V_{wd} is the wind speed 10 m above sea level; L_{pp} is the length between perpendiculars; and C_{xw}, C_{yw}, and C_{xyw} are the longitudinal, transverse, and yaw wind load coefficients, the values of which are given in the reference (Yang 2018).

For the components of the superstructure, the IMCA recommends using the application programming interface (API)

Table 3 Longitudinal projection area of component A_L

Components	Superstructure	Crane 1	Crane 2	Crane 3	Crane 4	Winch	Slide
A_L/m^2	277.17	7.124	7.124	7.124	7.124	35.364	3.204

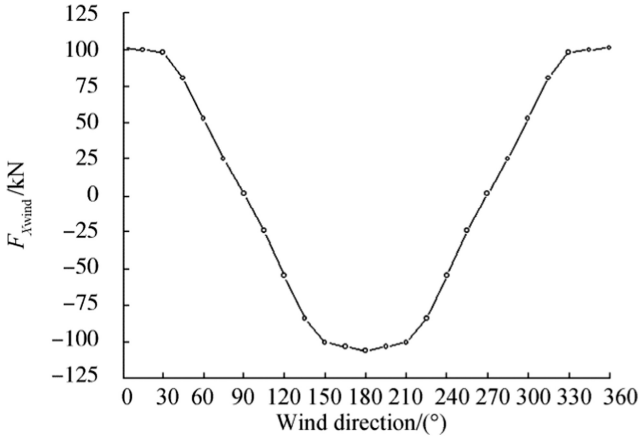

Fig. 4 Longitudinal wind load

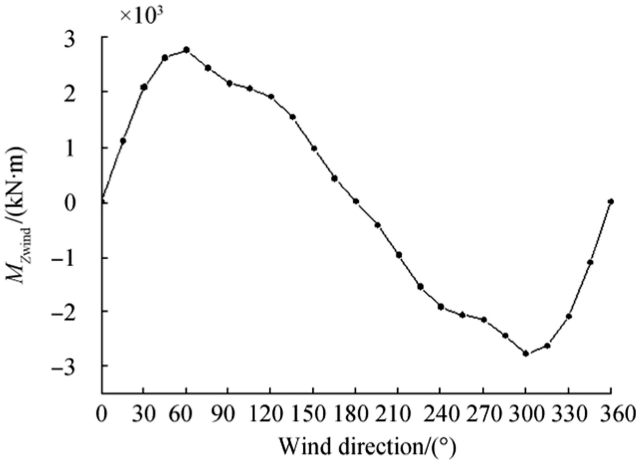

Fig. 6 Yaw wind load

method. The wind load of each shipboard component is determined by the size of its longitudinal and transverse projection areas and its shape and height coefficients. In essence, the API formula is also a kind of modular method, relative to the proposed ABS and DNV formulas (Yang 2018). The API formula differs by its use of interpolation to determine the wind direction of the module by the wind load. The wind load is calculated as follows:

$$\begin{cases} F_{\text{wdx}} = C_{\text{wd}}(C_{\text{s}}C_{\text{h}}A_{\text{T}})v_{\text{wd}}^2 \\ F_{\text{wdy}} = C_{\text{wd}}(C_{\text{s}}C_{\text{h}}A_{\text{L}})v_{\text{wd}}^2 \end{cases} \tag{2}$$

where C_{wd} is the wind load coefficient (0.615, when the force unit is kN); C_{s} is the shape coefficient; C_{h} is the height coefficient; A_{T} is the lateral projection area of the component, for which the calculation results for the CTV superstructure are shown in Table 2; and A_{L} is the longitudinal projection area of the component, for which the results are shown in Table 3, where v_{wd} is the wind speed 10 m above sea level, which we set to 17.1 m/s.

The wind load in any wind direction from 0 to 90° can be obtained by interpolation with respect to the wind loads at 0° and 90°. Similarly, the wind load in any wind direction from 90° to 180° can be obtained by interpolation with respect to the wind loads at 90° and 180°:

$$F_{\text{wd}}(\partial) = F_{\text{wdy}}(90)\left[\frac{2\sin^2(\partial)}{1+\sin^2(\partial)}\right] + F_{\text{wdx}}(0)\left[\frac{2\cos^2(\partial)}{1+\cos^2(\partial)}\right] \tag{3}$$

$$F_{\text{wd}}(\partial) = F_{\text{wdy}}(90)\left[\frac{2\sin^2(\partial)}{1+\sin^2(\partial)}\right] + F_{\text{wdx}}(180)\left[\frac{2\cos^2(\partial)}{1+\cos^2(\partial)}\right] \tag{4}$$

where ∂ is the wind direction angle; $F_{\text{wd}}(\partial)$ is the corresponding wind load; $F_{\text{wdx}}(0)$ is the longitudinal wind load when ∂ = 0°; $F_{\text{wdy}}(90)$ is the transverse wind load when ∂ = 90°; and $F_{\text{wdx}}(180)$ is the longitudinal wind load when ∂ = 180°. Since the total wind load in any wind direction can be determined using the parallelogram principle, we can obtain the longitudinal and transverse wind loads for any wind direction. The

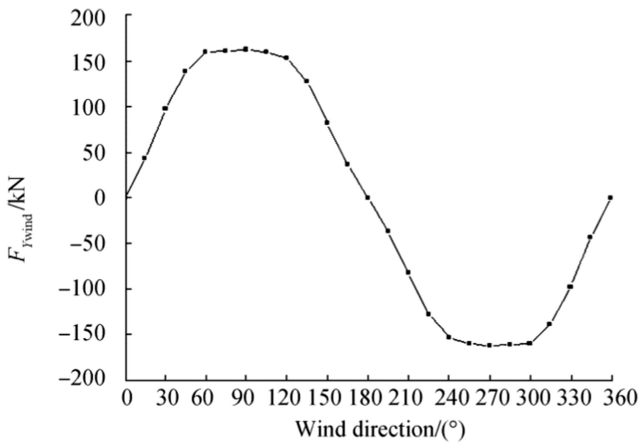

Fig. 5 Transverse wind load

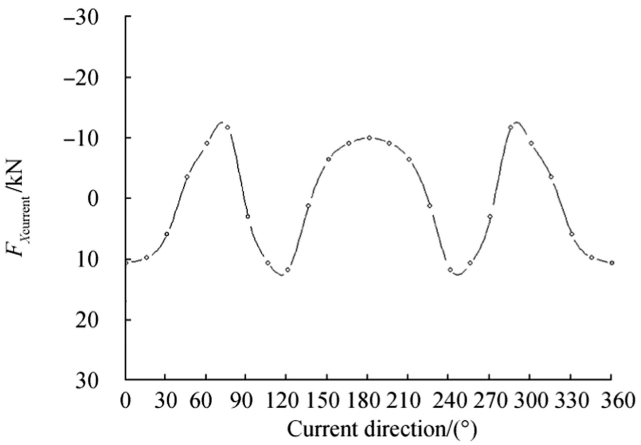

Fig. 7 Longitudinal current load

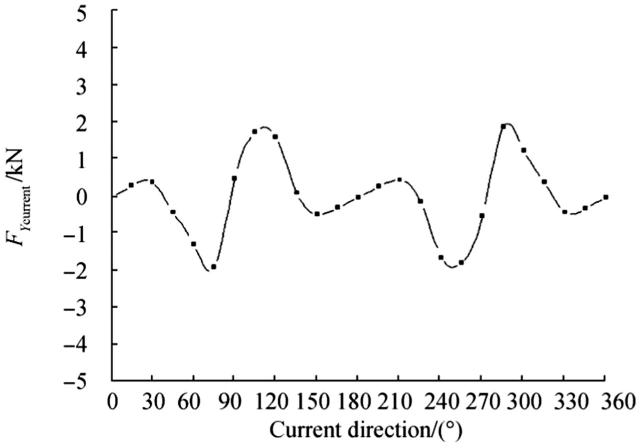

Fig. 8 Transverse current load

wind moment produced by the transverse force depends on the transverse force and the arm:

$$\begin{cases} F_{\text{wdx}}(\partial) = F_{\text{wd}}(\partial)\cos(\partial) \\ F_{\text{wdy}}(\partial) = F_{\text{wd}}(\partial)\sin(\partial) \\ F_{\text{wdz}}(\partial) = F_{\text{wdy}}(\partial)X_{\text{wdc}} \end{cases} \tag{5}$$

So, we can calculate the wind loads on the main hull and superstructure of the CTV. By superposing the wind load of these two CTV parts, we can obtain the wind load on the CTV in any wind direction. In this paper, we provide the longitudinal wind load ($F_{X\text{wind}}$), transverse wind load ($F_{Y\text{wind}}$), and yaw wind load ($M_{Z\text{wind}}$) for the CTV for wind directions ranging from 0 to 360° in 15° steps. Figures 4, 5, and 6 show the respective results.

3.2 Current Load

The current load on the CTV is much smaller than the wind load, so the current speed is generally regarded as having

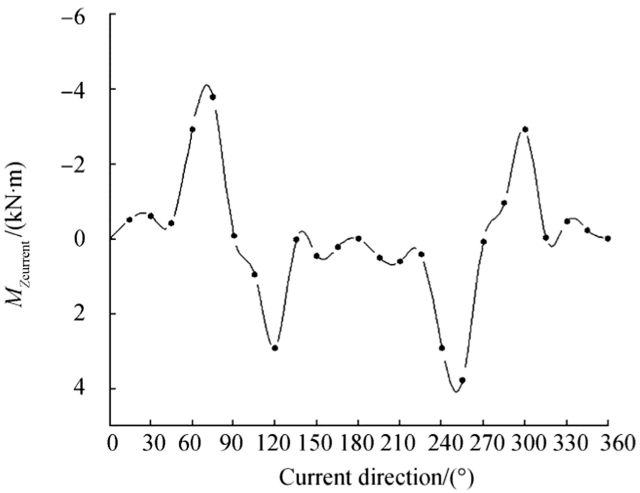

Fig. 9 Yaw current load

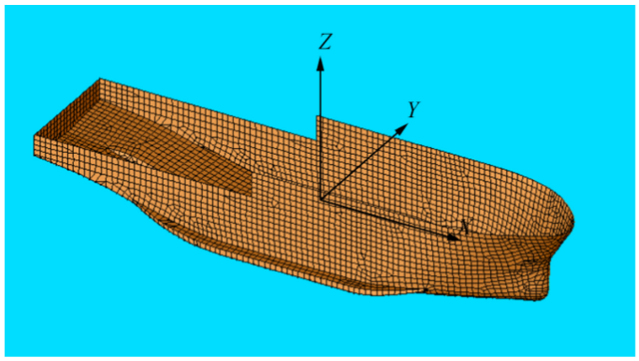

Fig. 10 CTV mesh model

constant velocity, and accordingly, the current load is usually regarded as constant. In this paper, we use the OCIMF method (OCIMF 1994) to calculate the current load on the CTV, for which the longitudinal, transverse, and yaw current loads are expressed as follows:

$$\begin{cases} F_{xc} = \dfrac{1}{2} C_{xc}\rho_c V_{cR}^2 T L_{PP} \\ F_{yc} = \dfrac{1}{2} C_{yc}\rho_c V_{cR}^2 T L_{PP} \\ M_{xyc} = \dfrac{1}{2} C_{xyc}\rho_c V_{cR}^2 T L_{PP}^2 \end{cases} \tag{6}$$

where ρ_c = 1025 kg/m^3 is the density of sea water; V_{cR} is the average current velocity; T is the mean draft of the ship; and C_{xc}, C_{yc}, and C_{xyc} are the longitudinal, transverse, and yaw current load coefficients, respectively.

We can determine the longitudinal current load ($F_{X\text{current}}$), transverse current load ($F_{Y\text{current}}$), and yaw current load ($M_{Z\text{current}}$) on the CTV in full load conditions as in the determination of the wind load. Figures 7, 8, and 9 show the calculation results.

3.3 Wave Load

In this paper, we use the commercial software AQWA to calculate the wave load. Figure 10 shows the CTV ship model.

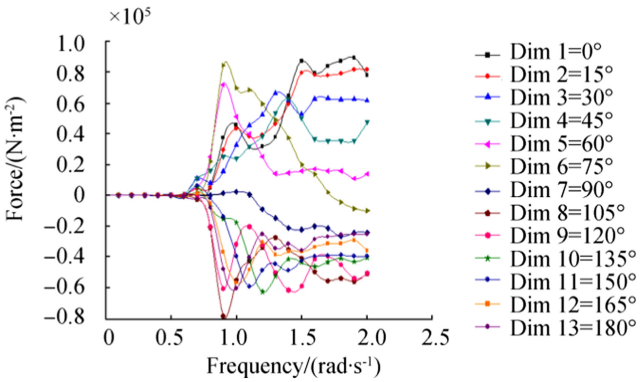

Fig. 11 Steady drift force of surge

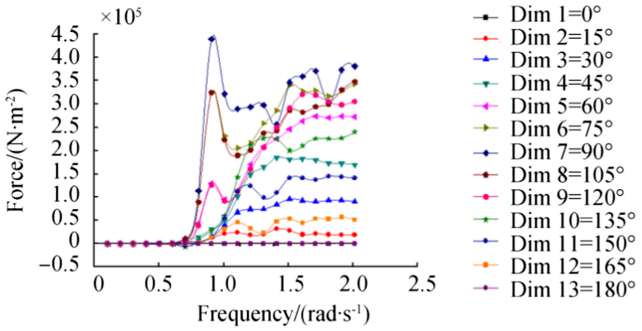

Fig. 12 Steady drift force of sway

We used the far-field method to calculate the response amplitude operator (RAO) of the CTV at different frequencies (0.1–2.0) and wave angles (0–180°) (Chen 2007), as shown in Figs. 11, 12, and 13. In these figures, the curve indicates the change in the second-order slow drift RAO in the frequency domain for different waves.

When the RAO of the wave load in regular waves has been obtained, we can obtain the wave load under irregular wave conditions. Using the spectral analysis method, we can obtain the second-order wave load of the CTV, the results of which are shown in Figs. 14, 15, and 16.

3.4 Total Environmental Load on the CTV

Having calculated the wind, current, and wave loads on the CTV in the DP mode, we can obtain the total environmental load on the CTV by summing these values, the results of which are shown in Figs. 17, 18, and 19.

3.5 External Load on a CTV Towing a VLCC

We must also determine the external load of the CTV when towing a VLCC and cruising at 2 kn near the FPSO. Because the CTV has a shielding effect on the VLCC, and considering the coupling effect, the resistances of the two ships should be less than the linear superposition of their resistances when they are in open seas. However, here, we focus on the maximum demand on the CTV DP ability. Therefore, to ensure optimal safety performance, we can exclude interaction between the two ships to ensure that the propeller provides adequate resistance to the external load of the thrust.

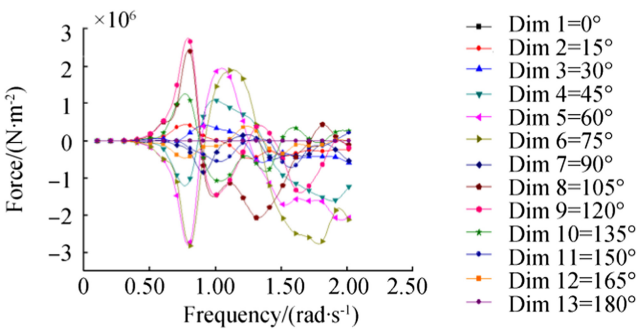

Fig. 13 Steady drift force of yaw

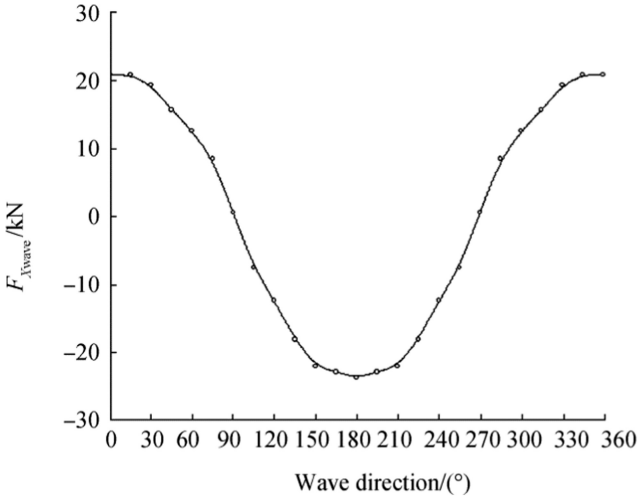

Fig. 14 Longitudinal second-order wave load

3.6 External Load in Self-propeller Mode

Although in this paper we mainly focus on a demand analysis of the positioning capability of the CTV, in practical applications, the DP propulsion device will operate in the positioning mode at lower inflow speed and in the migration mode at higher inflow speed to and from port. Therefore, it is necessary to analyze and consider the external loads for the navigation mode of the CTV.

3.6.1 Resistance in Calm Water

We use the Holtrop method to estimate the resistance in calm water, the results of which are shown in Table 4.

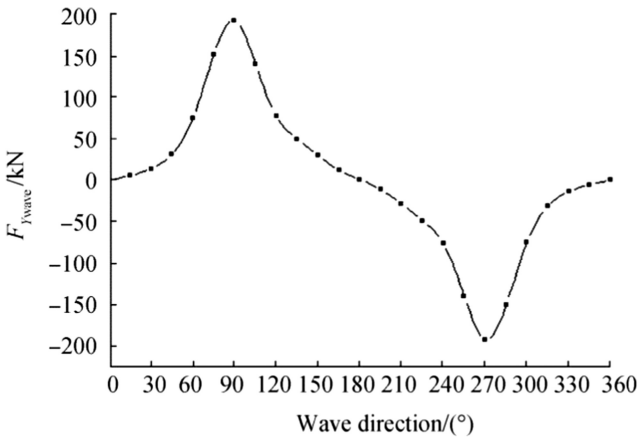

Fig. 15 Transverse second-order wave load

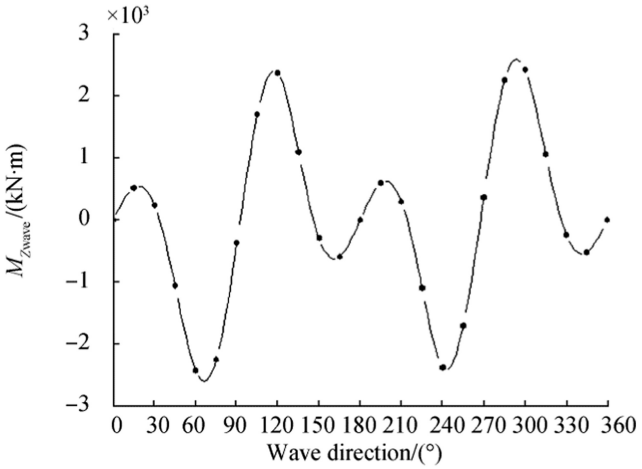

Fig. 16 Yaw second-order wave load

As we can see in the table, when the CTV is towing a VLCC at 2 kn, the water resistance in calm water is 61.1 kN.

3.6.2 Air Resistance

The air resistance can be expressed by the following formula:

$$R_{aa} = C_a \frac{1}{2} \rho S U^2 \tag{7}$$

where ρ = 1.226 kg/m^3 is the air density; S is the horizontal projection area of the main hull and the superstructure above the water surface; and U is the air speed relative to the main hull, $U = V + U_w \cos \phi$, and U_w is the wind speed. For our study of sea conditions, U_w = 17.1 m/s; V is the ship speed; and ϕ is the angle of the wind direction and the centerline of the ship, for which in this study we only consider ϕ = 180°.

Using Eq. (7), we can calculate the sum of the air resistance of the CTV towing a VLCC at a speed of 2 kn to be 124 kN.

So, the external load of a CTV towing a VLCC at a speed of 2 kn is 185.1 kN.

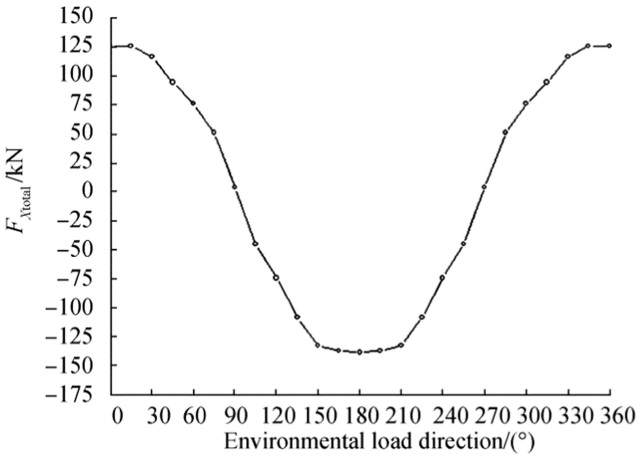

Fig. 17 Total longitudinal environmental load

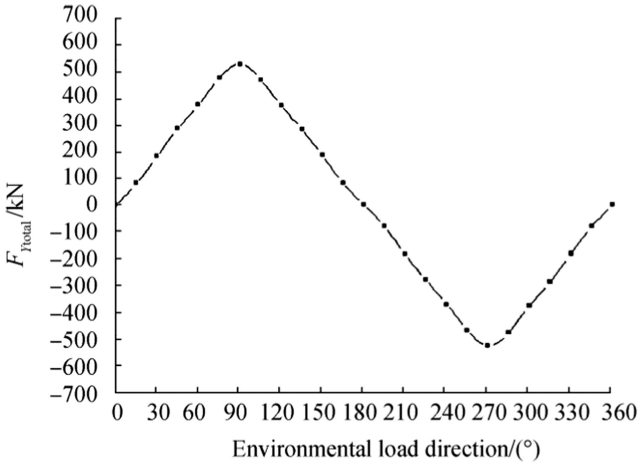

Fig. 18 Total transverse environmental load

4 Conclusions

The CTV, as an intermediate carrier of crude oil from an FPSO to a VLCC, must have the following capabilities: (1) an independent positioning capability to resist disturbances from wind, wave, and current loads; (2) the ability to position the VLCC and other ordinary tankers around the FPSO; (3) the ability to travel and navigate between the FPSO and ports. In this paper, we provided the three main application modes of the CTV through an analysis of the positioning capability requirements. We performed a theoretical analysis and calculated the wind, wave, and current loads and the navigation resistances of the CTV in the designed sea conditions. We then established a numerical prediction model of the CTV wave force based on the far-field integral theory in AQWA software. We calculated the second-order wave force RAO of the CTV in regular waves, then used spectral analysis to predict the second-order steady wave force of the CTV for different wave directions. The results show that the method proposed in this paper can be used to calculate the environment load. This

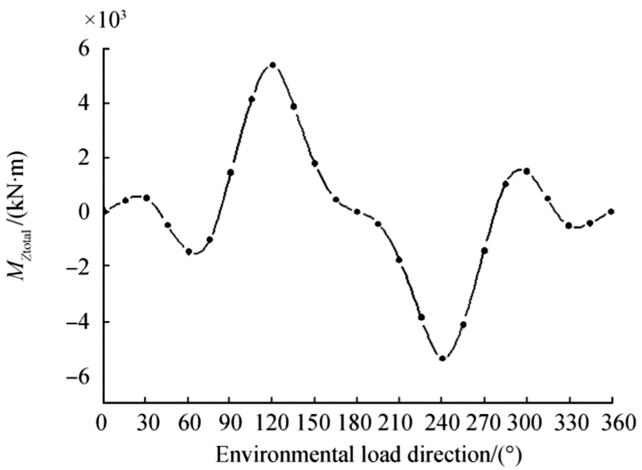

Fig. 19 Total yaw environmental load

Table 4 Resistance in calm water

Ship type	Ship speed/kn	R_{total}/kN
CTV	2	7.6
VLCC	2	53.5

research provides reference information for the design of the thrust and positioning systems of the CTV.

Funding This study is supported by the National Natural Science Foundation of China (Grant No. 51509046) and Foundation of Ministry of Industry and Information Technology High-tech Ship Scientific Research (Grant No. 2016-26).

References

Bao WE (2018) Research on time domain analysis of dynamic positioning system for drilling platform. Master thesis, Jiangsu University of Science and Technology, Zhenjiang, 9–22. (in Chinese)

Chen XB (2007) Middle-field formulation for the computation of wave-drift loads. J Eng Math 59(1):61–82. https://doi.org/10.1007/s10665-006-9074-x

Do KD (2011) Global robust and adaptive output feedback dynamic positioning of surface ships. J Mar Sci Appl 10:325–332. https://doi.org/10.1109/ROBOT.2007.364136

Fossen TI (1994) Guidance and control of ocean vehicles. Wiley Press, New York, pp 45–46

Fu MY, Ding FG, Zhang WX (2010) The ship capability calculation of a dynamic positioning system based on genetic algorithms. J Mark Q Publ Am Mark Assoc 73(6):920–925. https://doi.org/10.1109/ICCA.2010.5524471

Kjerstad ØK, Skjetne R (2014) Modeling and control for dynamic positioned marine vessels in drifting managed sea ice. Model Identif Control 35(4):249–262. https://doi.org/10.4173/mic.2014.4.3

Li MX, Ren XL (2018) Development of DP2 Marginal Oilfeld Shuttle Tankers. Guandong Shipbuilding 37(5):13-15+34 (in Chinese)

Liang H, Li L, Ou J (2015) Coupled control of the horizontal and vertical plane motions of a semi-submersible platform by a dynamic positioning system. J Mar Sci Technol 20(4):776–786. https://doi.org/10.1007/s00773-015-0322-5

Lin XG, Nie J, Jiao YZ (2018) Nonlinear adaptive fuzzy output-feedback controller design for dynamic positioning system of ships. Ocean Eng 158(15):186–195. https://doi.org/10.1016/j.oceaneng.2018.03.086

Liu ZF, Sun Q, Liu CD (2016) Thrust ability evaluation analysis of a dynamic positioning system. J Ship Mech 20(5):540–548. (in Chinese). https://doi.org/10.3969/j.issn.1007-7294.2016.05.004

Mahfouz AB (2007) Predicting the capability-polar-plots for dynamic positioning systems for offshore platforms using artificial neural networks. Ocean Eng 34(8):1151–1163. https://doi.org/10.1016/j.oceaneng.2006.08.006

Mahfouz AB, Eltahan HW (2006) On the use of the capability polar plots program for dynamic positioning systems for marine vessels. Ocean Eng 33(8):1070–1089. https://doi.org/10.1016/j.oceaneng.2005.08.006

OCIMF (1994) Prediction of wind and current loads on VLCCs. Witherby $ CO.LTD, London, pp 37–51

Sun LP, Liu Y, Li XP (2011) DP3 capability analysis of a semisubmersible drilling platform. Shipbuild China 52(4):100–108. (in Chinese). https://doi.org/10.1097/RLU.0b013e3181f49ac7

Tannuri EA, Morishita HM (2006) Experimental and numerical evaluation of a typical dynamic positioning system. Appl Ocean Res 28(2):133–146. https://doi.org/10.1016/j.apor.2006.05.005

Wang L, Yang JM, Xu SW (2018) Dynamic positioning capability analysis for marine vessels based on a DPCap polar plot program. China Ocean Eng 32(1):90–98. https://doi.org/10.1007/s13344-018-0010-4

Wu D, Liu X, Ren F, Yin Z (2016) An improved thrust allocation method for marine dynamic positioning system. Nav Eng J 129(3):35–44

Xin H, Du J (2018) Robust nonlinear control design for dynamic positioning of marine vessels with thruster system dynamics. Nonlinear Dynam 94(1):1–12. https://doi.org/10.1007/s11071-018-4364-1

Xu R, Wang Q, Song Y (2011) Study on ship dynamic positioning system's thruster allocation based on genetic algorithm. International Conference on Information Science & Technology, IEEE, Beijing. https://doi.org/10.1109/ICIST.2011.5765191

Xu SW, Wang L, Wang XF, Li B (2016) Experimental evaluation on a newly developed dynamic positioning time domain simulation program. J Ship Mech 20(6):686–698. https://doi.org/10.3969/j.issn.1007-7294.2016.06.005

Yang D (2018) Analysis on the marine traction positioning on the sea and the demand of the positioning capability. Master thesis, Harbin Engineering University, Harbin, 7–32. (in Chinese)

Zhang BW, Yang H (2009) Investigation on the methods used in the analysis of DP capability. Shipbuilding of China 50(s):205–214 (in Chineese)

Zhang YF, Liu CD, Zhang FW, Wang ZP (2016) Numerical evaluation on dynamic positioning for semisubmersible platform based on backstepping control. J Ship Mech 20(12):1547–1555. https://doi.org/10.3969/j.issn.1007-7294.2016.12.005

Zhao W (2018) Research on optimal control of thrust and power distribution in offshore engineering ship. Ship Sci Technol 40(10):87–92. https://doi.org/10.3404/j.issn.1672-7649.2018.10.017

Zhao DW, Ding FG, Tan JF (2010) Optimal thrust allocation based GA for dynamic positioning ship, International Conference on Mechatronics & Automation, IEEE, Xi'an. https://doi.org/10.1109/ICMA.2010.5589933